



# Propagation of waves in a layer of a viscoelastic material underlying a layer of a moving fluid<sup>☆</sup>



V.V. Vedeneev

*M.V. Lomonosov Moscow State University, Moscow, Russia*

## ARTICLE INFO

### Article history:

Received 2 December 2014

Available online 4 August 2016

## ABSTRACT

The motion of waves in a layer of a viscoelastic material of finite thickness with a layer of an ideal incompressible fluid moving over it is considered in connection with the problem of the turbulent friction reduction in a boundary layer by using compliant coatings. The dispersion equation is obtained, and the behaviour of its roots is analysed. It is proved that when the flow velocity exceeds a certain value, two types of instability appear: a weaker instability, which is caused by the viscous properties of the material and vanishes in the purely elastic case, and a stronger instability, which is present in the case of an elastic material. The stability criteria of short and long waves are found in analytical form, and it is shown numerically for both types of instability that among all wavelengths the smallest critical velocity is achieved on short waves, whose stability criterion thus gives the stability criteria of all waves. The resonance wavelengths at which the interface undergoes strictly vertical vibrations are analysed. A resonance wavelength equal to 3–5 thicknesses is scarcely influenced by the fluid; nevertheless, a second resonance with a wavelength equal to 5–20 thicknesses appears when the fluid is present. The results obtained are used to estimate the influence of a moving fluid on the effectiveness of compliant coatings used to reduce turbulent friction.

© 2016 Elsevier Ltd. All rights reserved.

## 1. Introduction

In a series of problems of practical importance a significant part of the drag of solid bodies moving in a fluid is created by the friction in the turbulent boundary layer. For example, for modern cargo ships it can be as high as 70% of the total drag. Among the methods for reducing turbulent friction, namely, active control of the surface vibration, the creation of regular structures (riblets) on the surface in the flow field, the use of porous surfaces with injection/suction from the boundary layer, the use of polymer additives, hydrophobic surfaces and the organization of ventilated cavitation for detaching the fluid from the body in the flow field, the use of compliant coatings can be singled out.

The influence of the compliance of the surface on which the boundary layer forms was first discovered experimentally by Kramer.<sup>1</sup> Many studies on the stability of laminar boundary layers on elastic and viscoelastic surfaces have been published.<sup>2–9</sup> It has been shown that the elastic and viscous properties of a surface have a significant influence on the form of the neutral curve and that, in addition, apart from inviscid instability and Tollmien–Schlichting instability, a series of new forms of instability related to the compliance of the surface has appeared.<sup>2–4</sup> A specific combination of surface properties enables the critical Reynolds number to be increased by more than two fold with an accompanying increase in the length of the laminar portion of the boundary layer.<sup>9</sup>

The influence of compliant coatings on turbulent boundary layers has been investigated to a far lesser extent. There are approaches of two types: those based on direct numerical simulation of a turbulent boundary layer on deformable surfaces<sup>10–12</sup> and those based on the use of simplified models and the development of qualitative criteria, whose fulfilment should result in lowering of the turbulent friction.<sup>13–15</sup> Despite the fact that the approaches of the former type give a better understanding of the physical mechanisms of friction reduction, the difficulties in the direct numerical simulation of turbulence still prevent obtaining reliable and practically convenient criteria of the effectiveness of coatings. On the other hand, some proposed criteria<sup>13,15</sup> have been confirmed by experimental data and are convenient

<sup>☆</sup> Prikl. Mat. Mekh. Vol. 80, No. 3, pp. 317–343, 2016.

E-mail address: [vasily@vedeneev.ru](mailto:vasily@vedeneev.ru)

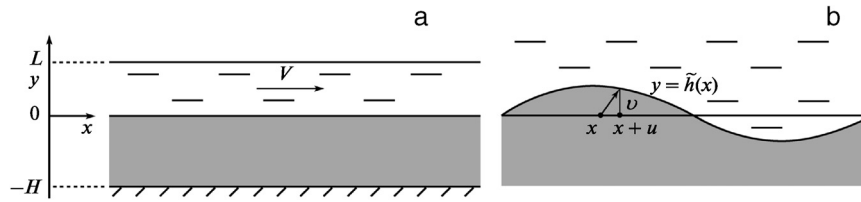


Fig. 1.

for practical use. In addition, they rely only on intrinsic parameters of coatings, such as the stiffness of the coating, the phase velocity, the frequency and the wavelength in the coating, which, in turn, are expressed in terms of properties of the material, making the use of these criteria convenient in practice. As a rule, these parameters are determined experimentally for specific materials by investigating the propagation of waves in a layer of the material immersed in air.<sup>15</sup> However, when a coating works in water, the propagation speeds of waves vary due to the inertia of the fluid, which has not heretofore been taken into account in the existing criteria.<sup>13,15</sup>

We stress that despite the fact that the coatings are intended to interact with a turbulent boundary layer, the proposed criteria<sup>13,15</sup> contain specifically the intrinsic wave velocities, which are measured or calculated without consideration of the boundary layer: it is assumed that the latter has practically no influence on the propagation speeds of the surface waves. Therefore, the boundary layer is also not taken into account in the formulation of the problem solved in this study.

The problem of the propagation of waves in compliant coatings immersed in a uniform fluid flow has been solved in several studies, but the coating itself was modelled as a plate on an elastic foundation.<sup>3,6,16,17</sup> Such a model does not take into account the shear strains in the elastic material and incorrectly reflects the dispersion properties of monolithic coatings, and it also does not describe the resonance phenomena in the elastic layer, which has been shown<sup>15</sup> to play a fundamental role. Several papers, in which the coating was simulated within the theory of elasticity,<sup>4,9,18,19</sup> take into account the boundary layer, making it necessary to use numerical methods and precluding an analytical investigation of the properties of the waves. In Ref. 18 absence of the boundary layer was considered as a special case; however, the thickness of the fluid layer was assumed to be infinite, and the investigation was also carried out numerically only for specific values of the parameters. Monographs 20 and 21 present results for waves in an elastic layer in contact with a layer of a fluid, but its motion is not taken into account.

**2. Statement of the problem**

We will investigate the behaviour of linear waves in a layer of a linearly elastic material of thickness  $H$  (the case of viscoelasticity reduces to the elasticity case by introducing complex elastic moduli and will be considered below), which is fastened on one side to an absolutely rigid plane, over which there is a layer of an inviscid incompressible fluid of thickness  $L$  (Fig. 1a). In the general case the fluid moves with the constant velocity  $V$  parallel to the interface. The gravity force is directed opposite to the  $y$  axis.

We introduce a system of coordinates with the  $x$  axis along the direction of motion of the fluid, as is shown in Fig. 1a. We will investigate two-dimensional motions in the  $x, y$  plane. We will first consider the equilibrium state of the system. Solving the equations of the linear theory of elasticity and hydrodynamics, we can easily show that it takes the following form: the layer of elastic material is in a compressed state under the action of its own weight and the weight of the fluid layer, and hydrostatic distributions of the pressure are established both in the fluid and in the elastic layer:

$$\begin{aligned}
 p^0 &= p_a + \rho_f g L - \rho_f g y, & 0 < y < L \\
 \sigma_{22}^0 &= -(p_a + \rho_f g L - \rho_f g y), & \sigma_{12}^0 &= 0, & -H < y < 0
 \end{aligned}
 \tag{2.1}$$

where  $\rho$  and  $\rho_f$  are the densities of the material and the fluid. We will assume that the displacement of the elastic-layer/fluid interface under the action of the weight of the fluid and the layer itself is a small quantity, which can be neglected.

We will consider the perturbations of the equilibrium state. Suppose  $\{u, v\}$  is the displacement vector of the elastic medium and  $\Phi$  is the potential due to the motion of the fluid. We introduce the functions  $\phi$  and  $\psi$  (Ref. 22, Chapter 9, Section 10), so that

$$u = \phi_x + \psi_y, \quad v = \phi_y - \psi_x
 \tag{2.2}$$

Then the equations of motion for perturbations of the elastic medium take the form (Ref. 22, Chapter 9, Section 10)

$$\Delta \phi - \frac{1}{a_1^2} \phi_{tt} = 0, \quad \Delta \psi - \frac{1}{a_2^2} \psi_{tt} = 0
 \tag{2.3}$$

Here  $a_1$  and  $a_2$  are the velocities of longitudinal and transverse waves in the elastic medium expressed in terms of the Lamé coefficients  $\lambda$  and  $\mu$ :

$$a_1 = \sqrt{\frac{\lambda + 2\mu}{\rho}}, \quad a_2 = \sqrt{\frac{\mu}{\rho}} \Rightarrow \lambda = \rho(a_1^2 - 2a_2^2), \quad \mu = \rho a_2^2$$

Expressions for the components  $\sigma_{22}$  and  $\sigma_{12}$  of the stress tensor are needed below. Expressing the components of the strain tensor in terms of displacement vector (2.2) and using Hooke's law, we obtain

$$\sigma_{22} = \lambda(\phi_{xx} + \phi_{yy}) + 2\mu(\phi_{yy} - \psi_{xy}), \quad \sigma_{12} = \mu(2\phi_{xy} + \psi_{yy} - \psi_{xx})
 \tag{2.4}$$

Below, instead of the Lamé coefficients  $\lambda$  and  $\mu$ , we will use the velocities of the longitudinal and transverse waves in the elastic medium  $a_1$  and  $a_2$  as the defining properties of the material.

The equation for the potential of an inviscid incompressible fluid is Laplace's equation

$$\Delta\Phi = 0 \tag{2.5}$$

The perturbation of the pressure is expressed in terms of the perturbation of the potential using the Cauchy–Lagrange integral, which is written in the linearized form as

$$p = -\rho_f(\Phi_t + V\Phi_x + gy) \tag{2.6}$$

where  $y$  is the vertical displacement of a particle of the fluid.

We will now formulate the boundary conditions, considering only small deviations of the elastic-layer/fluid interface and the free surface of the fluid from the unperturbed state. This enables us to state the corresponding boundary conditions on the unperturbed surfaces.

On the lower boundary of the elastic layer there should be zero displacements:

$$y = -H: u = v = 0 \tag{2.7}$$

On the elastic-layer/fluid interface three boundary conditions should hold. First, the equality between the normal and tangential components of the stress tensor gives two conditions:

$$y = 0: \sigma_{22} = -p, \quad \sigma_{12} = 0 \tag{2.8}$$

Second, the condition of impermeability through the deformed surface should hold on this surface. We note that the height of the boundary points, which appears in expression (2.6) for the pressure and in the impermeability condition, is given in the linear approximation of the function  $v(x, 0)$ . In fact, in the general case

$$\tilde{h}(x + u(x, 0)) = v(x, 0)$$

where  $y = \tilde{h}(x)$  is the equation of the interface (Fig. 1b). After linearization we obtain

$$\tilde{h}(x) = v(x, 0)$$

and the impermeability condition takes the form

$$y = 0: \Phi_y = Vv_x + v_t \tag{2.9}$$

The boundary condition on the free surface of the fluid is equality of the pressure to the atmospheric pressure, that is, equality of the pressure perturbation to zero:

$$y = L: p = -\rho_f(\Phi_t + V\Phi_x + gh) = 0 \tag{2.10}$$

Since the height of the level of the free surface appears in expression (2.10), it should be treated as the additional unknown function  $h(x, t)$ . The following kinematic impermeability condition should be written for it:

$$y = L: \Phi_y = Vh_x + h_t \tag{2.11}$$

### 3. Dispersion equation

We will consider the wave motions of the system:

$$(\phi, \psi, \Phi, h) = (f_1(y), f_2(y), s(y), c_0)e^{i(kx - \omega t)}$$

Then the equations of motion of the elastic medium (2.3) are written in the form

$$f_j'' - (k^2 - k_j^2)f_j = 0, \quad k_j = \omega/a_j \tag{3.1}$$

Here and below,  $j = 1, 2$ , and the prime sign denotes the derivative with respect to  $y$ . The equation of motion of the fluid (2.5) takes the form

$$s'' - k^2s = 0 \tag{3.2}$$

We will write the boundary conditions. When equalities (2.2) are taken into account, on the lower boundary of the elastic layer the condition of zero displacements (2.7) reduces to the following:

$$y = -H: f_1' - ikf_2 = 0, \quad f_2' + ikf_1 = 0 \tag{3.3}$$

On the elastic-layer/fluid interface equality (2.8) of the normal and tangential components of the stress tensor after linearization takes the form

$$y = 0: \sigma_{22} = -p = \rho_f(\Phi_t + V\Phi_x + gv), \quad \sigma_{12} = 0$$

The perturbation of the component  $\sigma_{22}$  is a sum of two parts. First, it changes due to the motion of the medium. This part is given by expression (2.4). Second, due to the change in the height of the interface, the unperturbed value of  $\sigma_{22}$  differs by  $\rho g v$  (2.1). Using expression (2.2) for  $v$ , we obtain

$$\begin{aligned} y = 0: & (a_1^2 - 2a_2^2)(f_1'' - k^2 f_1) + 2a_2^2(f_1'' - ikf_2') + g(f_1' - ikf_2) \\ & = im(kV - \omega)s + mg(f_1' - ikf_2), \quad f_2'' + 2ikf_1' + k^2 f_2 = 0; \quad m = \rho_f / \rho \end{aligned} \quad (3.4)$$

The condition of impermeability through the deformed surface (2.9) is written in the form

$$y = 0: s' = i(kV - \omega)(f_1' - ikf_2) \quad (3.5)$$

Finally, on the free surface of the fluid conditions (2.10) and (2.11) are rewritten as follows:

$$y = L: i(kV - \omega)s + gc_0 = 0, \quad s' = i(kV - \omega)c_0 \quad (3.6)$$

Thus, the system of equations (3.1) and (3.2) and boundary conditions (3.3)–(3.6) is a closed system.

The general solution of each of Eqs (3.1) and (3.2) is represented in the form of a linear combination of exponential functions:

$$\begin{aligned} f_j &= c_{j1} e^{\lambda_j y} + c_{j2} e^{-\lambda_j y}, \quad \lambda_j = \sqrt{k^2 - k_j^2} \\ s &= c_{31} e^{\lambda_3 y} + c_{32} e^{-\lambda_3 y}, \quad \lambda_3 = k \end{aligned} \quad (3.7)$$

Substitution into boundary conditions (3.3)–(3.6) produces a linear homogeneous system of seven equations containing the constants  $c_0$ ,  $c_{j1}$ ,  $c_{j2}$ ,  $c_{31}$  and  $c_{32}$ . Setting its determinant equal to zero, we obtain a dispersion equation that relates the wave number  $k$  and the phase velocity  $c = \omega/k$ .

For convenience in the further investigation, we first go over to dimensionless variables after selecting  $a_2$ ,  $H$  and  $\rho$  as the dimensional independent quantities that characterize the elastic layer. We bring the remaining quantities into dimensionless form in the following manner:

$$c' = \frac{c}{a_2}, \quad k' = kH, \quad a' = \frac{a_2}{a_1}, \quad V = \frac{V}{a_2}, \quad m = \frac{\rho_f}{\rho}, \quad L' = \frac{L}{H}, \quad g' = \frac{gH}{a_2^2} \quad (3.8)$$

where the prime signs denote dimensionless variables. Then, from the parameters of the elastic layer, only Poisson's ratio  $\nu$  remains, since the ratio

$$a' = \frac{a_2}{a_1} = \sqrt{\frac{1-2\nu}{2(1-\nu)}}$$

does not depend on Young's modulus and  $0 < a' < \sqrt{3}/2$ . Then the dispersion equation is written in the following dimensionless form (henceforth the prime signs are omitted until Section 10):

$$\begin{aligned} & \langle [(2 - c^2)^2 (\text{ch} k \alpha \text{ch} k \beta - (\alpha \beta)^{-1} \text{sh} k \alpha \text{sh} k \beta) \\ & + 4(\text{ch} k \alpha \text{ch} k \beta - \alpha \beta \text{sh} k \alpha \text{sh} k \beta) - 4(2 - c^2)] \\ & - (m - 1) g k^{-1} \beta^{-1} c^2 \{ \text{ch} k \alpha \text{sh} k \beta - \alpha \beta \text{sh} k \alpha \text{ch} k \beta \} \rangle (1 - g k^{-1} (V - c)^{-2} \text{th} k L) \\ & = m c^2 (V - c)^2 \beta^{-1} (\text{th} k L - g k^{-1} (V - c)^{-2}) [\text{ch} k \alpha \text{sh} k \beta - \alpha \beta \text{sh} k \alpha \text{ch} k \beta] \end{aligned} \quad (3.9)$$

Here

$$\alpha(c) = \sqrt{1 - a^2 c^2}, \quad \beta(c) = \sqrt{1 - c^2}$$

The problem is defined by five dimensionless parameters:  $a$ ,  $V$ ,  $m$ ,  $L$ ,  $g$ .

#### 4. Structure of the dispersion equation

Since dispersion equation (3.9) is cumbersome, we will examine its structure and evaluate the physical meaning of each factor. It can be written schematically in the form

$$\begin{aligned} & \langle [\text{waves on the surface of the material}] - (m - 1) g k^{-1} \beta^{-1} c^2 \{ \text{effect of gravity} \} \rangle \\ & \times (\text{waves on the surface of the fluid}) \\ & = m c^2 (V - c)^2 \beta^{-1} (\text{coupling - fluid}) [\text{coupling - material}] \end{aligned} \quad (4.1)$$

We will first assume that the right-hand side of this equation is equal to zero and examine the left-hand side, which consists of two factors, one in angle brackets and one in parentheses. The roots of the dispersion equation are given by the roots of each factor. The roots of the second factor have the form

$$c = V \pm \sqrt{\frac{g}{k} \operatorname{th} kL} \quad (4.2)$$

This is the dispersion relation for gravitational waves on the surface of a fluid of depth  $L$  with a fixed flat bottom (Ref. 23, Chapter 8, Section 11).

If we set  $g=0$ , the roots of the first factor are given by setting the expression in square brackets equal to zero. This is the dispersion equation for water on the surface of a layer of an elastic material of finite thickness in a vacuum.<sup>15</sup> When  $k \rightarrow \infty$  (when the thickness of the layer is infinite), the equation is transformed into the equation for Rayleigh waves on the surface of an elastic half-space (Ref. 22, Chapter 9, Section 10)

$$(2 - c^2)^2 - 4\alpha\beta = 0 \quad (4.3)$$

The term containing the factor in curly brackets in relations (3.9) and (4.1) clearly influences the surface waves in the elastic layer only when  $g \neq 0$  and thus expresses the effect of gravity. Physically, gravity plays the same role as in waves on the surface of a fluid: when the level of the surface of the elastic layer varies, the gravitational potential varies and, along with the elastic forces, causes the formation of waves. This term also vanishes when  $m = 1$ . Then the densities of the material and the fluid are equal, and a change in the position of the interface results in identical changes in the potentials in the material and the fluid. When  $m \neq 1$ , the potentials vary differently, causing the appearance of a surface wave, which is also expressed by this term.

We now turn to the right-hand side of the dispersion equation. It is equal to zero in the following cases.

*The case when  $L=0$ , i.e., absence of a fluid.* It is not difficult to see that the right-hand side decreases with the term from the left-hand side that is proportional to  $m$ .

*The case when  $m=0$ , i.e., the density of the fluid vanishes.* As was established above, there are two groups of roots. The roots of the first group, which describe waves on the surface of the material, are not influenced by the fluid owing to its non-inertial nature. The roots of the second group, which describe waves on the surface of the fluid, are not influenced by the layer, because its inertia becomes infinitely large in comparison to the inertia of the fluid, and the latter behaves as if the layer is non-deformable.

*The case when  $c=0$ , i.e., a standing wave in the system of coordinates connected to the elastic material.* The eigenfunction degenerates to a zero function, so that both the elastic layer and the fluid flow are in an unperturbed state. Therefore, their interaction vanishes.

If the gravity force is neglected ( $g=0$ ), the right-hand side vanishes also in the case when  $c=V$ , i.e., when the wave is standing relative to the fluid. Because of the absence of gravity, such a wave does not cause perturbations in the fluid; therefore, the perturbation of the pressure on the surface of the elastic medium is also equal to zero.

In the remaining cases the right-hand side is non-zero and clearly expresses the coupling of the waves on the surface of the material and on the surface of the fluid. The last factor contains only characteristics of the elastic layer, and the next-to-last factor contains only characteristics of the fluid layer, as is reflected in the structure of Eq. (4.1).

We note that when  $g=0$  and  $L \rightarrow \infty$ , dispersion equation (3.9) is identical to the equation obtained in Ref. 18 in the case of the absence of a boundary layer.

## 5. Characteristic behaviour of the waves

We will first consider the case in which the coating is oriented vertically, i.e., the gravity force acts parallel to the plane of the coating. Then the plane of Fig. 1a is horizontal, and the force of gravity does not act on the plane waves, i.e.,  $g=0$ . The results of the calculation of the phase velocity  $c$  (the solutions of Eq. (3.9) with the smallest absolute values) are presented below for the following values of the parameters:

$$v = 0.45 (\Rightarrow a = 0.302), \quad L = 100, \quad k = 2\pi/3 \quad (5.1)$$

and the dimensionless flow velocities  $V=0, 1, 2.2, 2.3$ . The wave number corresponds to a wavelength equal to the thickness of the layer times three. The left-hand side of Fig. 2 shows graphs of  $F_1(c) - F_2(c)$ , where  $F_1$  and  $F_2$  are the left-hand and right-hand sides of Eq. (3.9). The thick continuous curve corresponds to  $m=0$ , and the remaining curves correspond to  $m=1$  and the values of  $V$  indicated.

As is seen, the presence of the quiescent fluid significantly (by ~25%) decreases the phase velocities. When the flow velocity is non-zero, the graph becomes asymmetric: the velocity of the wave travelling along the flow increases, and the velocity of the wave travelling against the flow decreases. As  $V$  increases, the velocity of the wave travelling against the flow becomes zero, and then the wave is carried away by the moving fluid and becomes a wave travelling along the flow. When the velocity increases further, these two waves travelling along the flow merge into one, after which the corresponding two roots  $c(V)$  become complex-conjugate. Since one of them always has a positive imaginary part, instability of the elastic-medium/fluid interface in the form of travelling waves appears.

The right-hand side of Fig. 2 shows the dependence of the roots  $c(V)$  with the smallest absolute values which was calculated for parameter values (5.1) and  $m=1$  and illustrates the behaviour described above. Thus, the layer of elastic material can lose stability, if the fluid located above moves with a sufficiently large velocity.

We will now consider the case in which the coating is oriented horizontally, i.e., the force of gravity acts in the plane of Fig. 1a, and this plane is vertical.

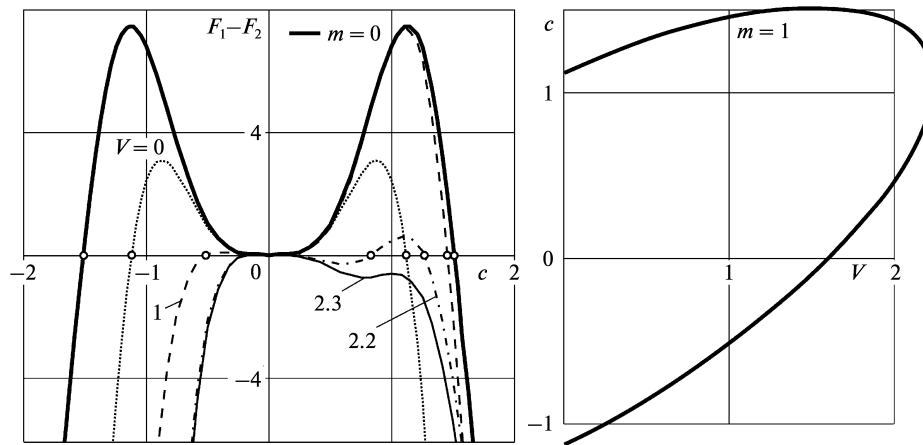


Fig. 2.

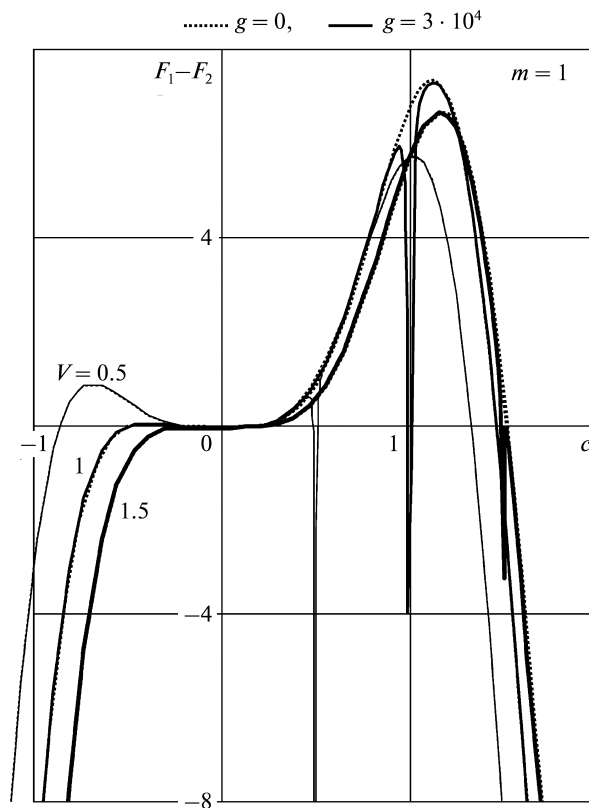


Fig. 3.

We will estimate the characteristic value of the dimensionless parameter  $g$ . For applications associated with compliant coatings (soft rubbers) the characteristic parameters of the material are: Young’s modulus  $E \approx 10^6$  Pa, and  $\rho \approx 10^3$  kg/m<sup>3</sup>. Then, the minimal value of the dimensional velocity is

$$a_2 = \sqrt{\frac{\mu}{\rho}} > \sqrt{\frac{E}{3\rho}} \approx 18 \text{ m/s}$$

We assume that  $H < 0.01$  m and the acceleration of free fall is equal to  $9.8$  m/s<sup>2</sup>. Then the value of the parameter is  $g < 3 \times 10^{-4}$ . In Eq. (3.9) it appears only in the combination  $g/k$ . We will consider wavelengths that do not exceed 100 thicknesses of the layer. Then the dimensionless wave number is  $k > 0.063$ . As a result, we have the ratio  $g/k < 0.005$ , and the terms with the multiplier  $g$  can always be neglected except in a small vicinity of the point  $c = V$ . In this vicinity there are two roots, which are close in magnitude to values (4.2) and correspond to gravitational waves on the surface of the fluid. The force of gravity has an even smaller influence in the case of more solid materials, including metals, due to the far greater value of the velocity  $a_2$ .

For the calculations we will take the largest characteristic value  $g = 3 \times 10^{-4}$ , and we will take the values of the remaining parameters, as before, in accordance with equalities (5.1). Figure 3 shows graphs of the difference  $F_1(c) - F_2(c)$  for  $m = 1$  and the dimensionless flow

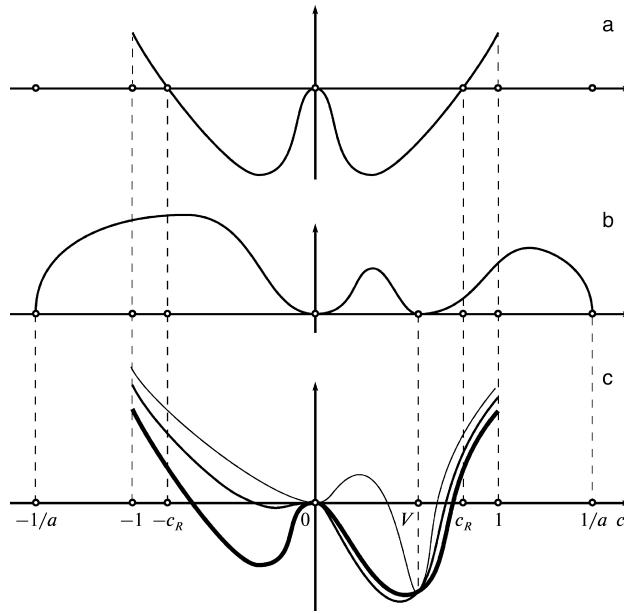


Fig. 4.

velocities  $V=0.5, 1.0, 1.5$ , which completely confirm the estimates performed (the dotted and solid lines correspond to  $g=0$  and  $g=3 \times 10^{-4}$ ). As can be seen, as opposed to the case when  $g=0$ , the graphs have downward directed narrow “peaks” in the vicinity of the point  $c=V$ , as a result of which two additional roots close to the value  $c=V$  appear. At the same time, outside of the vicinity of this point the graphs are practically indistinguishable from the analogous graphs for  $g=0$ .

Thus, when phase velocities corresponding to waves on a material/fluid interface are studied, as well when the stability is investigated, the influence of gravity can be neglected.

Below, for the investigation of the stability boundary, we need a dispersion equation in the form obtained after dividing both sides of Eq. (3.9) by  $\text{ch } k\alpha \text{ ch } k\beta$ :

$$\begin{aligned} & \langle [(2 - c^2)^2(1 - (\alpha\beta)^{-1} \text{th } k\alpha \text{ th } k\beta) + 4(1 - \alpha\beta \text{ th } k\alpha \text{ th } k\beta) - 4(2 - c^2)(\text{ch } k\alpha \text{ ch } k\beta)^{-1}] \\ & - (m - 1)gk^{-1}\beta^{-1}c^2 \{ \text{th } k\beta - \alpha\beta \text{ th } k\alpha \} \rangle (1 - gk^{-1}(V - c)^{-2} \text{th } kL) \\ & = mc^2(V - c)^2\beta^{-1}(\text{th } kL - gk^{-1}(V - c)^{-2})[\text{th } k\beta - \alpha\beta \text{ th } k\alpha] \end{aligned} \tag{5.2}$$

**6. Stability of short waves**

We will first examine the behaviour of short waves ( $k \rightarrow \infty$ ) in three velocity ranges:

- 1)  $|c| < 1$  ( $\alpha$  and  $\beta$  are real and, without loss of generality, positive numbers),
- 2)  $1 < |c| < 1/a$  ( $\alpha$  is positive, and  $\beta$  is purely imaginary),
- 3)  $|c| > 1/a$  ( $\alpha$  and  $\beta$  are purely imaginary).

We will investigate the first case. In Eq. (5.2) we go to the limit as  $k \rightarrow \infty$ , assuming that its roots  $c(k)$  then tend to finite non-zero values (the case in which  $c \approx 0$  will be considered below). In the present case we have the limiting value  $|c| < 1$ , i.e., the functions  $\alpha(c)$  and  $\beta(c)$  are real (and to be specific) positive. We obtain the equation

$$\langle [(2 - c^2)^2(1 - (\alpha\beta)^{-1}) + 4(1 - \alpha\beta)] \rangle = mc^2(V - c)^2\beta^{-1}[1 - \alpha\beta] \tag{6.1}$$

Its three roots are obvious:

$$\alpha\beta = 1 \Rightarrow c = 0, \pm\sqrt{1 + 1/a^2}$$

The root  $c=0$  gives a trivial solution, and the other two roots do not satisfy the condition  $|c| < 1$ . The remaining  $c$  roots of Eq. (6.1) are identical to the roots of the equation

$$((2 - c^2)^2 - 4\alpha\beta) + mc^2(V - c)^2\alpha = 0 \tag{6.2}$$

The first term on its left-hand side is identical to the left-hand side of (4.3) and has the roots  $c=0, \pm c_R$ , where  $c_R < 1$  is the phase velocity of the Rayleigh wave. The second term is negative and has the roots  $c=0, V, \pm 1/a$ . Graphs of the first and second terms on the left-hand side of (6.2) are shown in Figs 4a and 4b. In Fig. 4c the thick, ordinary and thin lines show their sum in the case when  $V < c_R$  for small, medium and large values of  $m$ .

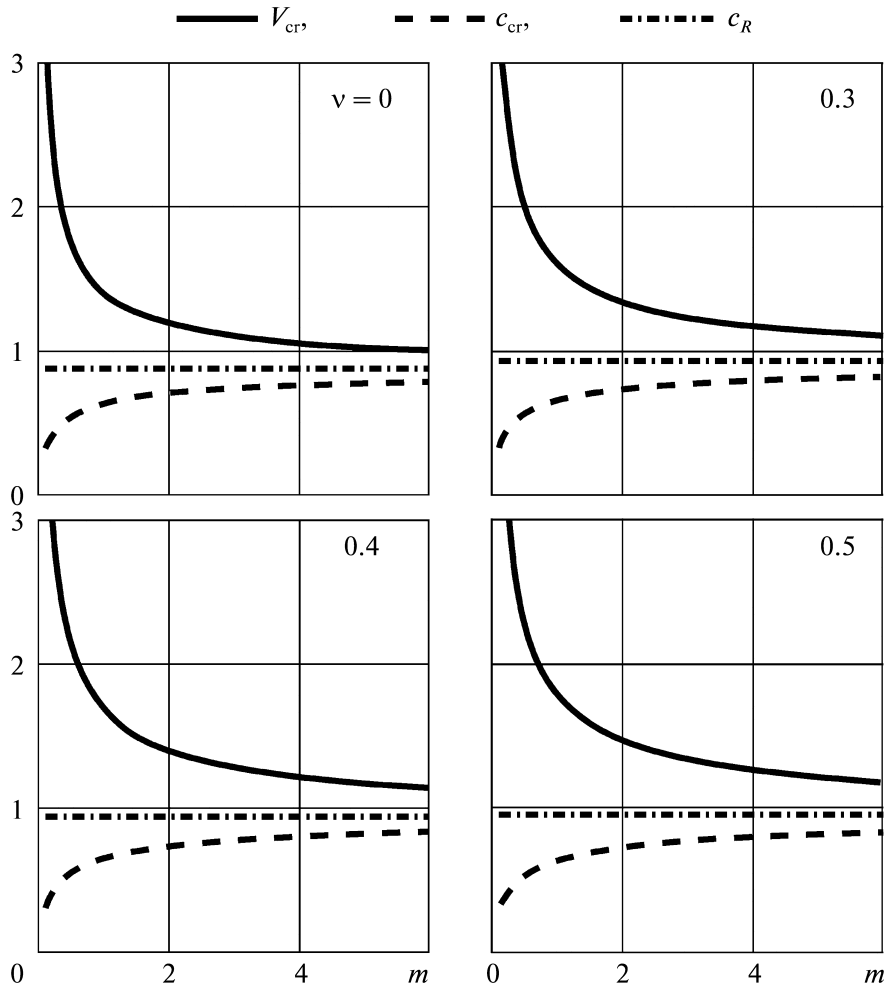


Fig. 5.

We will now fix the flow velocity  $V$  and increase the density of the fluid  $m$ . Then, in accordance with the graphs in Fig. 4c, the negative root  $c$  shifts to the right and becomes positive. The positive root decreases. If  $V < c_R$ , the situation illustrated in Fig. 4c by the thin line will take place at some large value of  $m$ . Since the left-hand side of Eq. (6.2) is negative for  $c = V$  and positive for  $c = 1$  and positive  $c \approx 0$ , there will be one root in each of the ranges  $0 < c < V$  and  $V < c < 1$ , and they will both tend to  $V$  as  $m \rightarrow \infty$ . If  $V > c_R$ , at sufficiently large  $m$  the two roots will become closer and merge, after which the entire left-hand side of Eq. (6.2) will become positive for  $0 < c < 1$ . A pair of complex conjugate roots, one of which has a positive imaginary part and will cause instability, then forms.

Thus, the following has been proved:

- 1) when  $V < c_R$ , merging of the roots and a transition to instability with short waves and  $|c| < 1$  is impossible at any  $m$ ,
- 2) when  $V > c_R$ , there is a fluid density  $m = m_{cr}(V)$ , which is such that short waves with  $|c| < 1$  are stable at  $m \leq m_{cr}$  and are otherwise unstable,  $m_{cr}(V) \rightarrow \infty$  as  $V \rightarrow c_R + 0$ , and the phase velocity  $c_{cr}$  at the instant of merging always satisfies the condition  $0 < c_{cr} < c_R$ .

A graph of the function  $V_{cr}(m)$  (the function which is the inverse of  $m_{cr}(V)$ ) is plotted numerically in Fig. 5 for several characteristic values of Poisson's ratio  $\nu$  (which determine the dimensionless parameter  $a$ ). The figure shows the dependence  $c_{cr}(m)$ , i.e., the value of the phase velocity at which merging of the roots and the transition to instability occur. The dash-dot line shows the value of the phase velocity of the Rayleigh wave  $c_R$ . For the case when  $m = 1$ , which is of greatest practical importance, and various values of  $\nu$  we obtain

$\nu$	0.0	0.3	0.4	0.45	0.5
$V_{cr}$	1.401	1.606	1.692	1.740	1.793
$c_{cr}$	0.631	0.654	0.650	0.644	0.635

Next, we will consider the roots  $c$  which satisfy the condition  $1 < |c| < 1/a$  when  $k \rightarrow \infty$ . In such a case the function  $\beta(c)$  becomes purely imaginary, and the corresponding hyperbolic tangent is transformed into the trigonometric tangent. More specifically, as  $k \rightarrow \infty$ , dispersion equation (5.2) is transformed into the following equation:

$$\langle [(2 - c^2)^2 (1 - (\alpha\beta')^{-1} \text{th} k\beta') + 4(1 + \alpha\beta' \text{tg} k\beta')] \rangle$$

$$= mc^2(V - c)^2(\beta'^{-1} \text{tg} k\beta' - \alpha)$$

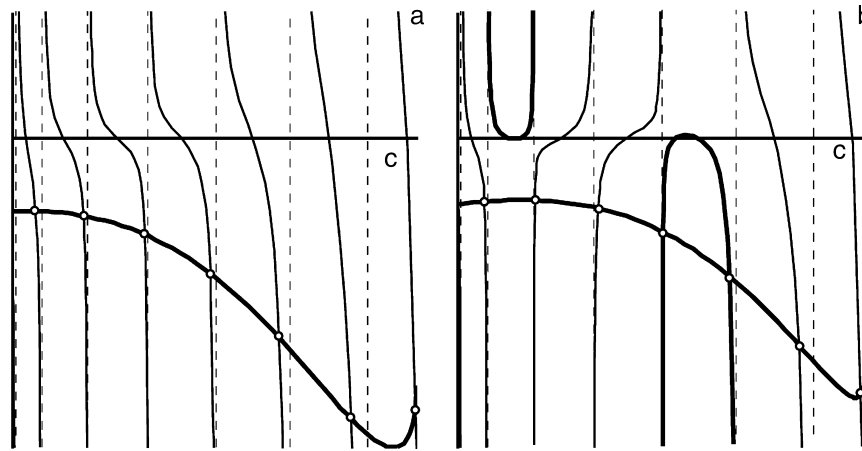


Fig. 6.

where  $\beta'(c) = \sqrt{c^2 - 1}$ . We rewrite it in the form

$$\frac{\text{tg } k\beta'}{\alpha\beta'} (- (2 - c^2)^2 + 4\alpha^2\beta'^2 - mc^2(V - c)^2\alpha) = - (2 - c^2)^2 - 4 - mc^2(V - c)^2\alpha \tag{6.3}$$

We will first consider the case when  $m = 0$ . The right-hand side of the equation is negative. The multiplier in parentheses on the left-hand side can be negative on the segment  $|c| \in [1, 1/a]$  or have the two roots  $|c| = c_{1,2}$ ,  $1 < c_1 < c_2 < 1/a$ , between which it is positive and negative in the opposite case. In the case of a negative multiplier, the graphs of the left-hand side and the right-hand side (the thick lines) of Eq. (6.3) on the segment  $|c| \in [1, 1/a]$  are shown in Fig. 6a. The equation has one root on each periodicity segment of the tangent, regardless of the value of the right-hand side. Non-zero values of  $m$  clearly only decrease the multiplier, causing variation of the roots, but not an interaction between them. A transition to instability is then obviously impossible.

Now, when  $m = 0$ , suppose we have an interval  $(c_1, c_2)$ , on which the multiplier in parentheses on the left-hand side of (6.3) is positive, that is, the graph of the entire left-hand side has two “loops”, which correspond to the roots  $c_{1,2}$ , as is shown in Fig. 6b (the loops are shown as thick lines). Since the tangent behaves here like  $1/(k\beta')$  near the asymptotes, at large  $k$  the loops between the two roots deviate to a negligibly small extent from zero, and thus they can be considered sign-invariant. In such a case the two roots correspond to one of the loops when  $m = 0$ , and no root corresponds to the other loop. When  $m$  is increased, the right-hand side of the equation decreases without changing sign, and the roots  $c_{1,2}$  of the left-hand side merge and vanish. This corresponds to the approach of the two loops toward one another and their disappearance, after which the qualitative form of the left-hand side corresponds to Fig. 6a and then does not change at any  $m$ . It is clear that since the right-hand side is always negative, during the approach and disappearance of the loops and even more so afterwards, interaction of the roots and a transition to instability are impossible.

Finally, we will consider the case of the phase velocities  $|c| > 1/a$ . We will use the dispersion equation in the form (3.9) and, after replacing the hyperbolic functions by trigonometric functions, when  $k \rightarrow \infty$ , we obtain the equation

$$\begin{aligned} & \langle [(2 - c^2)^2 (\cos k\alpha' \cos k\beta' - (\alpha'\beta')^{-1} \sin k\alpha' \sin k\beta') \\ & + 4(\cos k\alpha' \cos k\beta' - \alpha'\beta' \sin k\alpha' \sin k\beta') - 4(2 - c^2)] \rangle \\ & = mc^2(V - c)^2\beta'^{-1} [\cos k\alpha' \sin k\beta' + \alpha'\beta' \sin k\alpha' \cos k\beta'] \end{aligned}$$

where

$$\alpha'(c) = \sqrt{a^2c^2 - 1} > 0, \quad \beta'(c) = \sqrt{c^2 - 1} > 0$$

We will multiply it by  $2\alpha'\beta'$  and transform it. We first rewrite the left-hand side in the form

$$\begin{aligned} & A_{1+} \cos(k(\alpha' + \beta')) - A_{1-} \cos(k(\alpha' - \beta')) - C \\ & A_{1\pm} = (2 - c^2)^2 + 4\alpha'^2\beta'^2 \pm (2 - c^2)^2\alpha'\beta' \pm 4\alpha'\beta', \quad C = 8\alpha'\beta'(2 - c^2) \end{aligned}$$

We will prove that

$$|A_{1+}| > |A_{1-}| + |C| \tag{6.4}$$

Then in each segment between a minimum and a maximum of  $\cos(k(\alpha' + \beta'))$  the left-hand side of the dispersion equation has at least one root. It is obvious that  $A_{1+} > 0$ , i.e.,  $|A_{1+}| = A_{1+}$ . Next, we will consider two cases:  $A_{1-} \geq 0$  and  $A_{1-} < 0$ . In the former case we have

$$A_{1+} > A_{1-} + 8\alpha'\beta'|2 - c^2|$$

which is equivalent to

$$\alpha' \beta' (|2 - c^2| - 2)^2 > 0$$

In the latter case in a similar manner we obtain

$$(|2 - c^2| - 2\alpha' \beta')^2 > 0$$

In both cases we arrive at valid inequalities. Thus, inequality (6.4) is proved.

Now we bring the right-hand side into the form

$$A_{2+} \sin(k(\alpha' + \beta')) - A_{2-} \sin(k(\beta' - \alpha')), \quad A_{2\pm} = mc^2(V - c)^2 \alpha' (1 \pm \alpha' \beta')$$

Thus, the entire dispersion equation is rewritten in the form

$$A_+ \cos(k(\alpha' + \beta') + \varphi_1) - A_- \cos(k(\beta' - \alpha') + \varphi_2) - C = 0$$

$$A_{\pm} = \sqrt{A_{1\pm}^2 + A_{2\pm}^2} \quad (6.5)$$

where  $\varphi_1(c)$  and  $\varphi_2(c)$  are certain functions. From inequality (6.4) and the fact that  $|A_{2+}| > |A_{2-}|$  it follows that

$$|A_+| > |A_-| + |C| \quad (6.6)$$

Then, on each segment between a maximum and a nearby minimum of  $\cos(k(\alpha' + \beta') + \varphi_1)$  Eq. (6.5) has at least one root. It is not difficult to prove that there is only one on each segment, since  $k$  is a large number. In such a case all the roots are separated from one another by maximum and minimum points of the function  $\cos(k(\alpha' + \beta') + \varphi_1)$  and cannot interact and produce an instability. As a result, it has been proved that the instability appearing when  $k \rightarrow \infty$  can occur only when  $|c| < 1$ .

## 7. Stability of long waves

Unlike short waves, for which the influence of gravity vanished, in the case of very long waves, the gravitational terms are generally significant. However, it was shown in Section 5 that taking them into account is practically meaningless, because at all wavelengths which should generally be considered, these terms are negligibly small. Thus, we will set  $g=0$ , understanding that the word “long” refers to waves which are such that their length is much greater than the thickness of the layer, but, on the other hand, is not so great that it would be necessary to take into account the gravitational terms.

We will evaluate the influence of the thickness of the fluid layer  $L$ , which appears in the dispersion equation only in the form  $th\ kL$ . Since this function differs from unity by less than 1% when  $kL > 2.65$  and since  $k > 0.063$  when waves whose length does not exceed 100 thicknesses are considered, to rule out the influence of  $L$  it is sufficient to require that  $L > 42$ . In practice, waves whose wavelength is not greater than 5–10 thicknesses of the layer are mainly of interest, and the influence of  $L$  for them vanishes when the fluid layers are far thinner.

Thus, below we will assume that the thickness of the fluid layer is sufficiently large for all the wavelengths considered, so that  $th\ kL$  can be replaced by unity. As a result, the dispersion equation is reduced to the following:

$$\begin{aligned} & (2 - c^2)^2 (\operatorname{ch} k\alpha \operatorname{ch} k\beta - (\alpha\beta)^{-1} \operatorname{sh} k\alpha \operatorname{sh} k\beta) \\ & + 4(\operatorname{ch} k\alpha \operatorname{ch} k\beta - \alpha\beta \operatorname{sh} k\alpha \operatorname{sh} k\beta) - 4(2 - c^2) \\ & = mc^2(V - c)^2 \beta^{-1} [\operatorname{ch} k\alpha \operatorname{sh} k\beta - \alpha\beta \operatorname{sh} k\alpha \operatorname{ch} k\beta] \end{aligned} \quad (7.1)$$

We go to  $k \rightarrow 0$  in it, assuming that  $c(k) \rightarrow \infty$ . We obtain

$$(2 - c^2)^2 + 4 - 4(2 - c^2) = 0 \Rightarrow c^4 = 0$$

Thus, apart from the trivial solution, the remaining roots increase without limit when  $k \rightarrow 0$ . This enables us to simplify dispersion equation (7.1). We will take into account that  $\alpha(c)$  and  $\beta(c)$  become purely imaginary and that the hyperbolic functions become trigonometric. In the dispersion equation we discard the terms of order less than  $c^3$ , while retaining the terms with  $V$ ,

$$c^4 \operatorname{ch} k\alpha \operatorname{ch} k\beta = mc^2(V - c)^2 \beta^{-1} \operatorname{ch} k\alpha \operatorname{sh} k\beta - mc^2(V - c)^2 \alpha \operatorname{sh} k\alpha \operatorname{ch} k\beta$$

or, dividing by  $\operatorname{ch} k\alpha$  and taking into account that  $\beta \approx ic$  and  $\alpha \approx iac$ , we obtain

$$\left( \frac{c}{ma(V - c)^2} - \operatorname{tg} kac \right) \operatorname{cos} kc = \frac{\sin kc}{ac^2} \quad (7.2)$$

We will first examine the first approximation after setting the right-hand side equal to zero. Some of the roots are given by the expression

$$\operatorname{cos} kc = 0 \Rightarrow c_n \approx \frac{1}{k} \left( \frac{\pi}{2} + \pi n \right), \quad n \in \mathbb{Z} \quad (7.3)$$

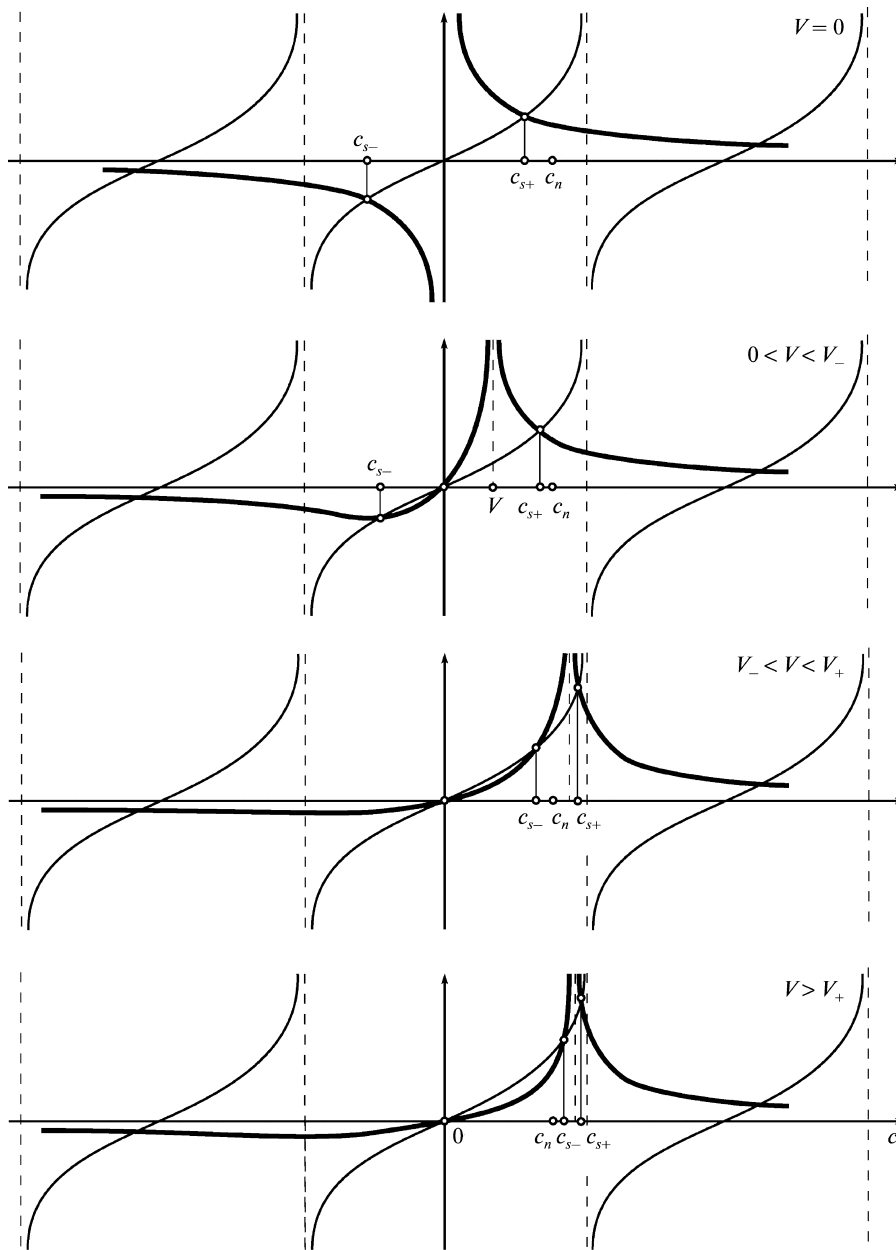


Fig. 7.

The remaining roots satisfy the equation

$$\operatorname{tg} kac = \frac{c}{ma(V-c)^2} \tag{7.4}$$

In this case, on each interval

$$\frac{1}{ak} \left( \frac{\pi}{2} + \pi s \right) < c_s < \frac{1}{ak} \left( \frac{\pi}{2} + \pi(s+1) \right), \quad s \in \mathbb{Z} \tag{7.5}$$

apart from  $s = -1$ , when  $V < \pi/(ak)$ , there is exactly one root for Eq. (7.4). Since they are isolated from one another, merging and a transition to instability are possible only upon interaction with roots of family (7.3).

We will find the minimal velocity  $V$  at which these roots are identical. For this purpose, we substitute expression (7.3) into Eq. (7.4) and solve it for  $V$ :

$$V = \frac{1}{k} \left( \frac{\pi}{2} + \pi n \right) \pm \frac{1}{\sqrt{k}} \sqrt{\frac{\pi/2 + \pi n}{ma \operatorname{tg}(a(\pi/2 + \pi n))}} \tag{7.6}$$

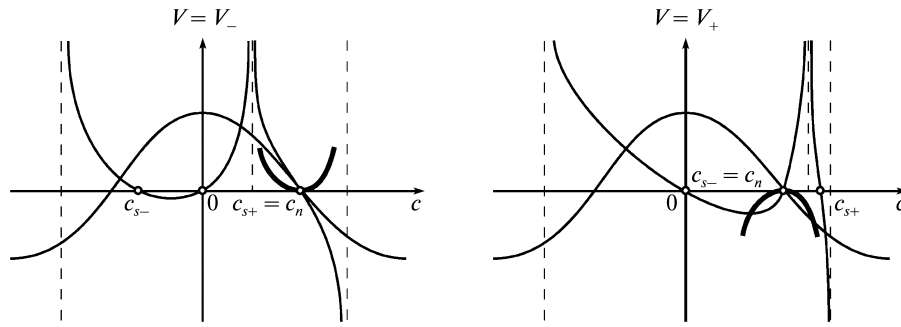


Fig. 8.

At small  $k$  the minimal values of  $V$  are achieved when  $n=0$ , i.e.,

$$V_{\pm} = \frac{1}{k} \frac{\pi}{2} \pm \frac{1}{\sqrt{k}} \sqrt{\frac{\pi/2}{\text{matg}(a\pi/2)}} \tag{7.7}$$

We will ascertain the physical meaning of the roots that are identical at  $V_{\pm}$ . Graphs of the left-hand (thin lines) and right-hand (thick lines) sides of Eq. (7.4) as the value of  $V$  increases are shown in Fig. 7. It is seen that

- a) when  $V=0$ , there are two roots of Eq. (7.4) with small absolute values, which increase with increasing  $V$ .
- b) when  $V=V_-$ , the positive root of Eq. (7.4) is equal to the smallest root of family (7.3) and continues to increase with increasing  $V$ .
- c) the negative root becomes positive, and when  $V=V_+$ , it is equal to the smallest root of family (7.3).
- d) subsequently, when  $V>V_+$ , it also continues to increase.

Thus, when  $V=V_-$ , the waves which travel downstream when  $V=0$  merge, and when  $V=V_+$ , the waves which travel upstream and downstream merge. It can be shown that only the latter merging results in instability when  $V=V_+$ .

To prove this we will consider the following approximation to the dispersion equation, taking into account the right-hand side of equality (7.2), which is always positive when the roots merge, so that the stability is determined by the sign of the left-hand side in the vicinity of  $c=c_n$  when  $V=V_{\pm}$ . Using Fig. 7, we easily construct a graph of the left-hand side of equality (7.2). Figure 8 shows graphs of each factor on the left-hand side (thin lines) and their product (thick lines) for the flow velocity  $V=V_-$  (left-hand side of Fig. 8) and  $V=V_+$  (right-hand side of Fig. 8). As is seen, in the case when  $V=V_-$ , in which the branches corresponding to the downstream travelling waves merge, the left-hand side in the vicinity of  $c=c_n$  is positive, and the roots remain real, i.e., there is no transition to instability. However, in the case when  $V=V_+$ , the left-hand side is negative in this vicinity. This indicates the presence of an interval of velocities  $V_+ - \varepsilon < V < V_+ + \varepsilon$ , where the real roots vanish, producing a complex-conjugate pair, i.e., instability. It is similarly proved that in the case when  $V < V_+ - \varepsilon$ , other possible matches of the roots of family (7.3) with roots of Eq. (7.4) in the intervals (7.5) with  $s \neq -1$  do not lead to instability.

Thus,  $V_+$  is the critical velocity, at which long waves become unstable.

### 8. Behaviour of waves in the vicinity of $c=0$

It was shown above that merging of the phase velocities of the waves with a transition to instability occurs between waves which move downstream and upstream when  $V=0$ . Before the transition to instability, i.e., when  $V < V_{cr}$ , the phase velocity of the upstream travelling wave passes through zero, where it intersects with the solution of Eq. (7.1)  $c=0$ , which always exists. We will investigate the behaviour at the time when the roots intersect and find the velocity  $V_0$  at which the phase velocity of the upstream travelling wave becomes zero. For this purpose we will examine Eq. (7.1) in the vicinity of  $c=0$ . Expanding the functions appearing in it according to Taylor's formula with accuracy to  $c^4$ , we obtain

$$c^4(k^2(1-a^2)^2 + 1 + \text{sh}^2 k(1-a^4)) = c^4 \frac{m}{2} (V-c)^2 (\text{sh} k \text{ch} k(1+a^2) - k(1-a^2)) \tag{8.1}$$

Thus, the root  $c=0$  has fourth-order multiplicity and does not interact with other roots that pass through this point. Reducing by  $c^4$ , we find the velocity at which the upstream travelling wave passes through  $c=0$  and becomes a downstream travelling wave:

$$V_0(k) = \sqrt{\frac{2(1-a^2)^2 k^2 + 1 + (1-a^4) \text{sh}^2 k}{m(1+a^2) \text{sh} k \text{ch} k - (1-a^2)k}}$$

It is not difficult to prove that the numerator and denominator in the second fraction under the radical are positive for any  $k$ .

Since we always have  $V_0(k) < V_{cr}(k)$ , the inequality  $V < V_0(k)$  can serve as a sufficient stability condition for waves with an assigned wavelength.

Calculations for the entire range  $0 < a < \sqrt{3}/2$  show that the minimum of  $V_0(k)$  is achieved when  $k \rightarrow \infty$  and is equal to

$$V_{0\min} = \sqrt{\frac{2(1-a^4)}{m(1+a^2)}}$$

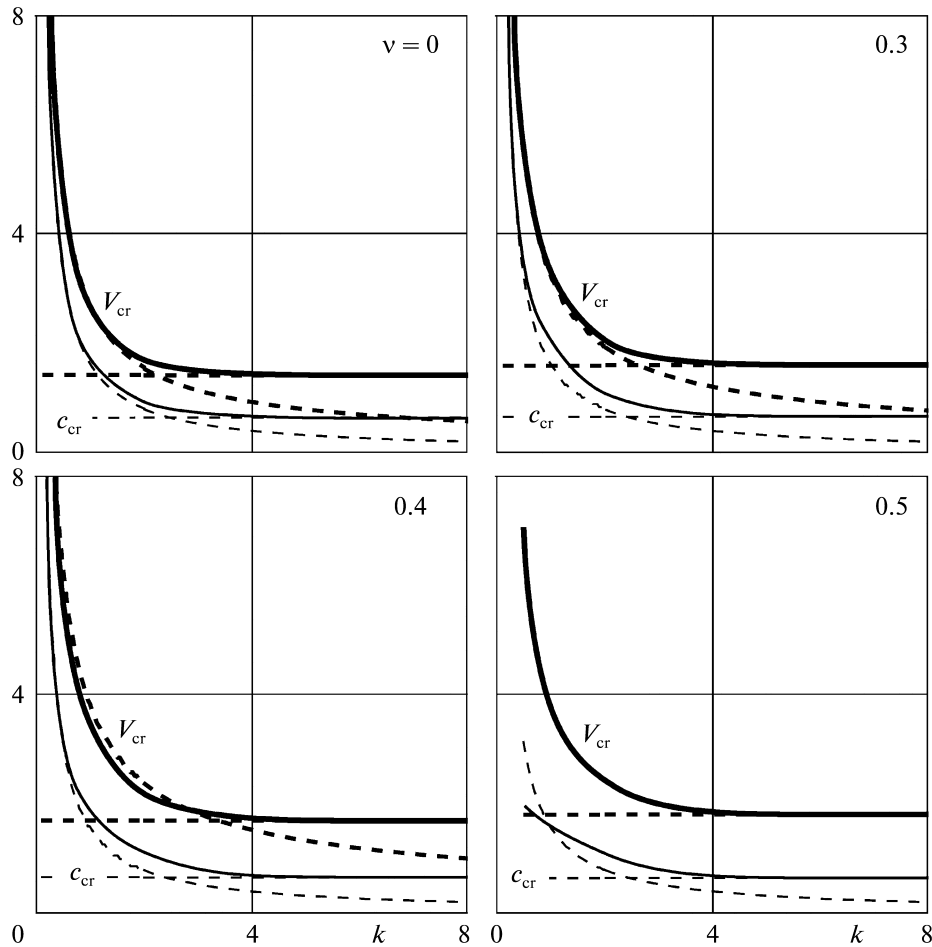


Fig. 9.

**9. Intermediate wavelength values**

In view of the complexity of dispersion equation (7.1), it could not be investigated analytically at arbitrary values of  $k$ ; therefore, a numerical analysis was performed. Newton’s method for systems of equations was used to solve two equations with respect to  $V_{cr}$  and  $c_{cr}$ : Eq. (7.1) and the same equation differentiated with respect to  $c$ . The smallest root with respect to  $V$  that corresponds to a non-zero value of  $c$  was sought. The calculations were performed for  $m=1$  and the values  $\nu=0, 0.3, 0.4, 0.5$ . The results are presented in Fig. 9, in which the graphs of  $V_{cr}(k)$  and  $c_{cr}(k)$  are shown as thick and thin lines, respectively. The asymptotic values of  $V_{cr}(k)$  and  $c_{cr}(k)$  for  $k \rightarrow 0$  and  $k \rightarrow \infty$  are indicated by the dashed lines.

As is seen, the numerical values approach the asymptotic values when  $k \rightarrow 0$  and  $k \rightarrow \infty$  (with the exception of the case when  $k \rightarrow 0$  and  $\nu=0.5$ , in which  $a=0$  and  $V_+$  becomes infinitely large). The minimum of  $V_{cr}(k)$  is achieved when  $k \rightarrow \infty$  in all the cases considered. This enables the values of  $V_{cr}$  from the graphs in Fig. 5 to be used as the minimum critical values with respect to  $k$ , below which the system is stable.

**10. Influence of the viscoelastic properties of the material on the stability**

Under harmonic vibrations, the viscoelastic properties of the material cause the appearance of imaginary parts of the elastic moduli, which depend in the general case on the frequency of the vibrations. Experiments have shown<sup>24</sup> that in this case Poisson’s ratio  $\nu$  remains real with a high accuracy, and only Young’s modulus becomes complex:

$$E = E_0(1 - 2i\omega\varepsilon(\omega)), \quad \varepsilon(\omega) = \delta(\omega)/E_0$$

where  $\delta(\omega)>0$  is the viscosity coefficient, which we will assume to be a small quantity compared with  $E_0/\omega$ . It was shown in Ref. 18 in an example of specific parameters of the problem that a small viscosity has a destabilizing effect on a downstream travelling wave at flow velocities at which it becomes an upstream travelling wave, i.e., at  $V>V_0(k)$ . We will prove this in the general case.

We will first evaluate the influence of the viscosity of the medium on the velocity  $a_2$ :

$$a_2 = \sqrt{\frac{\mu}{\rho}} = \sqrt{\frac{E}{2\rho(1+\nu)}} = \sqrt{\frac{E_0}{2\rho(1+\nu)}} \sqrt{1 - 2i\omega\varepsilon(\omega)} \approx a_{20}(1 - i\omega\varepsilon(\omega))$$

Thus, the quantity  $a_2$ , which was taken as the scale for the transition to the dimensionless quantities (3.8), becomes complex, and it is consequently expedient to evaluate the influence of the viscosity on the damping of waves in dimensional form.

In this section we will again mark the dimensionless quantities with a prime sign. Since the dimensionless parameter  $a'$  depends only on  $\nu$ , it remains real, and the only dimensionless parameter that is influenced by the viscosity is the dimensionless velocity  $V' = V/a_2$ . Then we obtain

$$c = c'(V'(a_2))a_2$$

Hence it is seen that when  $V=0$  (a quiescent fluid), the dimensionless phase velocities do not depend on the viscosity and are real. This corresponds to damped vibrations in dimensionless form.

We will investigate the influence of the viscosity when  $V \neq 0$ . For this purpose we calculate the derivative

$$\left. \frac{dc}{d\varepsilon} \right|_{\varepsilon=0} = -ia_{20}\omega \frac{dc}{da_2} = -ia_{20}\omega \left( c' - \frac{dc'}{dV'} V' \right) = -ia_{20}^2 k \left( c'^2 - V' c' \frac{dc'}{dV'} \right) \tag{10.1}$$

We find that the damping or growth of the waves in the presence of a small viscosity is determined by the positive or negative value of the expression  $c'^2 - V' c' dc'/dV'$  calculated without taking into account the viscosity. This enables us to use the results of the preceding sections for the analysis. For the upstream travelling wave corresponding to the phase velocity with the smallest absolute value, this expression is positive when  $V < V_0(k)$ , since  $V' > 0$ ,  $c < 0$ , and  $dc'/dV' > 0$ , i.e., this wave is damped. When  $V = V_0(k)$ , it vanishes (because  $c' = 0$ ), and it becomes negative when  $V > V_0(k)$ . Thus, at the flow velocity corresponding to the disappearance of the upstream travelling wave and its conversion into a downstream travelling wave, the damping of the wave is replaced by its growth under the action of the viscoelastic properties of the coating. We note that the replacement of the damping of the vibrations by their growth under the effect of a small viscosity also takes place at complex values of  $\nu$ , and the only difference will be in expression (10.1), which will also contain the derivative  $dc'/da'$ ; however, the entire expression will also change sign when  $c' = 0$ .

Thus, the instability caused by the viscosity that was discovered in Ref. 18 for a specific set of parameters also occurs in the general case. On the one hand, this instability sets in prior to the instability in the elastic case ( $V_0(k) < V_{cr}(k)$ ), and, on the other hand, it is weaker, and the rates of growth of the vibrations tend to zero when  $\varepsilon \rightarrow 0$ . A similar effect of destabilization of an upstream travelling wave by the viscosity at the flow velocity at which it becomes a downstream travelling wave also takes place in the simpler model of a compliant coating in the form of a plate on an elastic foundation.<sup>3</sup> It is assumed that instability caused by the viscosity is manifested in practice in the form of static deformation of the coating, i.e., divergence, while the “elastic” instability has a vibrational character, i.e., is flutter.<sup>3,18</sup>

The replacement of the damping of a wave by its growth and vice versa in all the remaining cases (i.e., when  $c' \neq 0$ ) takes place when the sign of the expression  $(c'/V') - (dc'/dV')$  changes. We will restrict ourselves here to an analysis of short waves and phase velocities of very small absolute value, for which calculations of the  $c'(V')$  curves reveal upward convexity for a downstream travelling wave and downward convexity for an upstream travelling wave (Fig. 2). It follows from equality (8.1) for an upstream travelling wave that  $dc'/dV' = 1$  when  $V = V_0$ , and from the results of Section 6 it follows that  $c'/V' < 1$  when  $V = V_{cr}$ . Then, from the downward convexity we obtain  $(c'/V') - (dc'/dV') < 0$  in the range  $V_0 < V < V_{cr}$ , i.e., this wave continues to be a growing wave in the case of a small viscosity until the main “elastic” instability appears. For an upstream travelling wave it is sufficient to consider the segment  $0 < V' < c'_R$ , where the function  $c'(V')$  increases, since on the segment  $c'_R < V' < V_{cr}$  it decreases, and the viscosity cannot result in intensification of the waves. After using Eq. (6.2), we can express the function  $V'(c)$  and show that  $dV'/dc' > 1$  when  $V' = 0$ . Therefore, we have  $dc'/dV' < 1$ . At the same time,  $c' = V'$  when  $V' = c'_R$  (Section 6), i.e., when  $c'/V' = 1$ . Then from the upward convexity we reason that on the entire segment  $0 < V' < V_{cr}$  the viscosity of the material causes damping of the downstream travelling wave.

As an example, Fig. 10 shows graphs of the real and imaginary parts of  $c/a_{20}$  as functions of  $V/a_{20}$  with parameters (5.1),  $m = 1$  and  $g = 0$  for various values of  $\varepsilon a_2/H$ .

### 11. Analysis of resonance wavelengths

For each solution of the dispersion equation  $c(k)$  there exists an eigenfunction, i.e., a non-zero solution of the system of linear equations for  $c_0, c_{j1}, c_{j2}, c_{31}, c_{32}$  (Section 3). This solution was found numerically.

As the relative amplitude of the vertical displacement of the upper surface of the elastic layer we will use the quantity

$$r = \left| \frac{v}{u} \right| = \left| \frac{\lambda_1 c_{11} - \lambda_1 c_{12} - ikc_{21} - ikc_{22}}{ikc_{11} + ikc_{12} + \lambda_2 c_{21} - \lambda_2 c_{22}} \right|$$

Only the first mode, which corresponds to a downstream travelling wave, is considered. For the case when  $m = 0$ , graphs of  $r(k/(2\pi))$ , where  $k/(2\pi) = H/\lambda$  is the ratio of the thickness of the layer to the wavelength, are shown on the left-hand side of Fig. 11. The results are the same as the known results.<sup>15</sup> As can be seen, when  $\nu > 0$ , there is a resonance wavelength equal to 3–4 thicknesses, for which practically all the surface energy is spent on the vertical displacement of the surface of the elastic layer. It was shown experimentally in Ref. 15 that the amplitude of the waves in the coating and its influence on the flow are most significant at the resonance wavelengths. The modification of  $r$  upon the appearance of a quiescent fluid ( $V=0$ ) and an increase in its density is given in the example of the case when  $\nu = 0.3$  on the right-hand side of Fig. 11. It is seen that besides the fundamental peak, whose position scarcely changes, a second resonance peak, which corresponds to a wavelength equal to 5–20 thicknesses (depending on  $m$ ), appears. The second peak is observed in the presence of the fluid in all the cases considered except  $\nu = 0.5$  (Fig. 12).

Calculations of  $r(k/(2\pi))$  in the presence of a moving fluid with velocities up to  $V_{cr}$  are shown in Fig. 12 for various values of  $\nu$ . The calculations were performed for  $m = 1$ . It is seen that the position of the “main” peak with  $\lambda \approx 3H$  scarcely varies, while the movement of the second peak is somewhat more significant. The results obtained show that the fundamental resonance wavelength scarcely depends on the rate of motion of the fluid and its density.

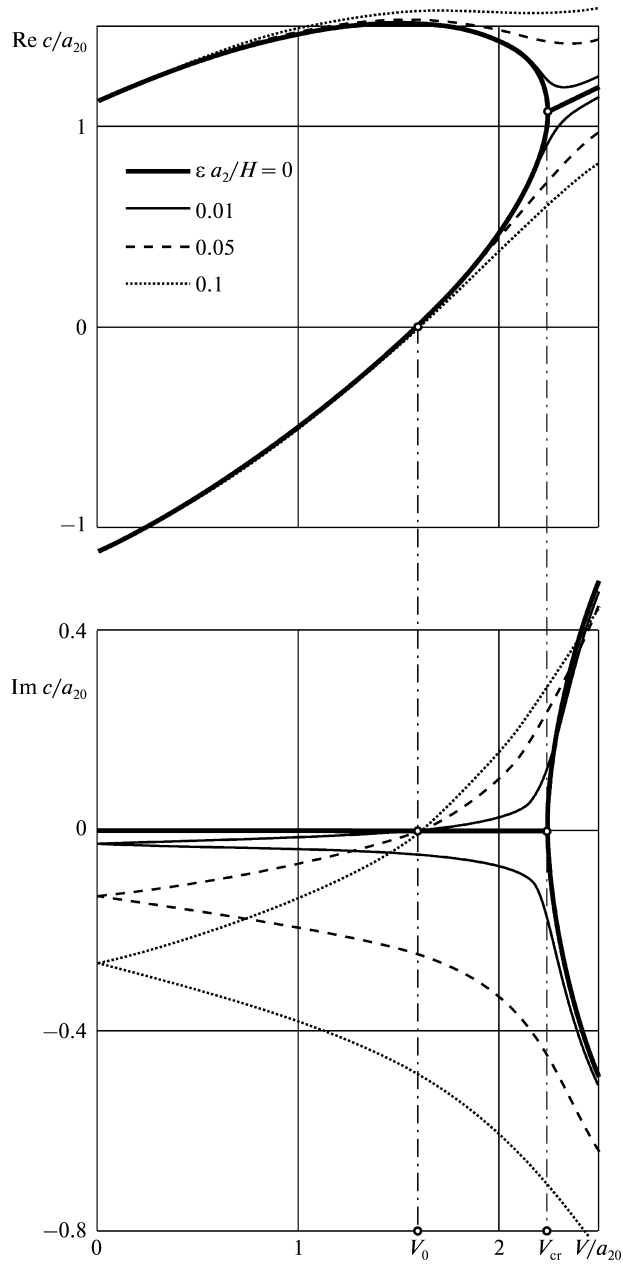


Fig. 10.

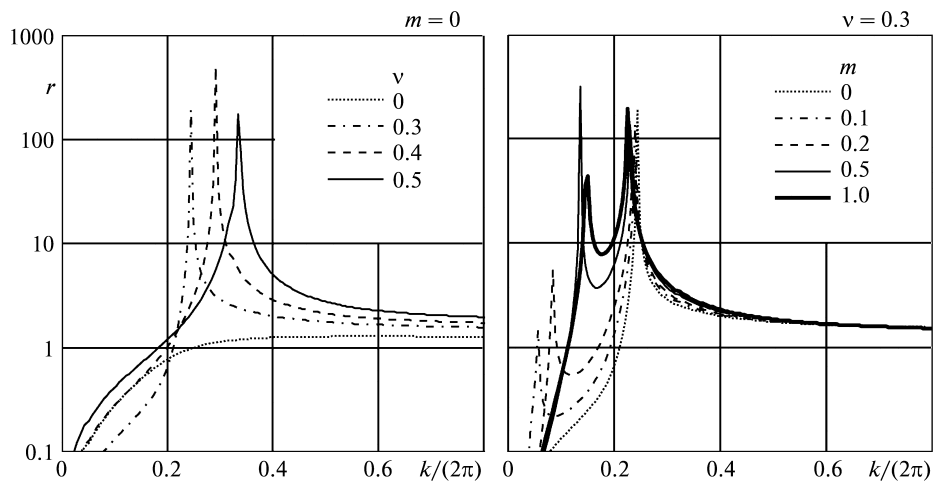


Fig. 11.

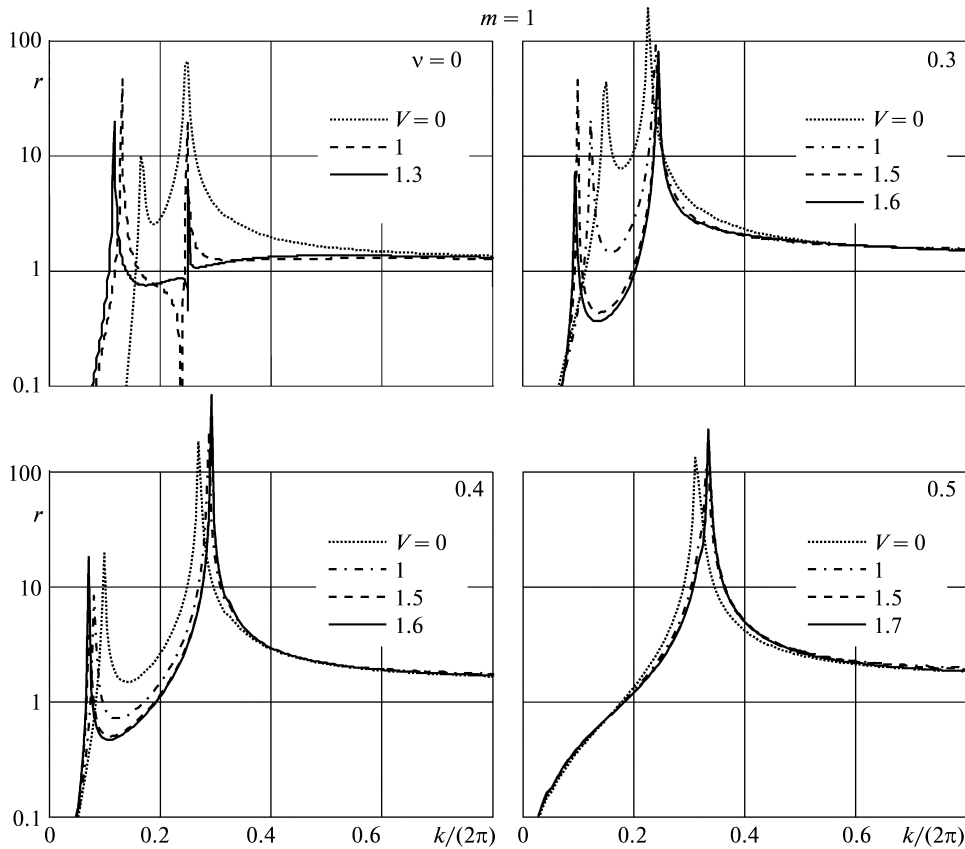


Fig. 12.

**12. Modification of the method for choosing coatings**

In accordance with the existing results,<sup>15</sup> the following criteria must be satisfied to ensure optimal interaction of the coating with the turbulent boundary layer:

- 1) the vibrational frequency must lie in the range<sup>25</sup>

$$6.67 \times 10^{-3} < \frac{f\nu_f}{u_\tau^2} < 2.00 \cdot 10^{-2}$$

Here  $f = \omega/(2\pi)$  is the physical dimensional vibrational frequency,  $\nu_f$  is the kinematic viscosity of the fluid, and  $u_\tau = \sqrt{\tau_w/\rho}$  is the boundary-layer scale of the velocity. Its dimensionless form is

$$6.67 \times 10^{-3} < \frac{c(k)k}{2\pi u_\tau^2} \frac{\nu_f}{Ha_2} < 2.00 \cdot 10^{-2} \tag{12.1}$$

- 2) the phase velocity must correspond to the velocity of motion of the turbulent structures:  $c(k) = (0.7 \dots 0.9)V$ ,
- 3) the coating must optimally influence the pressure pulsations, and for this reason the wavelength must be close to the resonance value:  $\lambda \approx 3H$ , i.e.,  $k \approx 2.09$ .

It was shown above that when  $m \neq 0$ , instability can appear. It must be avoided to maintain the effectiveness of the coating. Thus, one more condition is added:

- 4) the condition of hydrodynamic stability of the coating:

$$V < V_{cr}$$

The criterion of stability used here is the criterion of “elastic” stability: when such instability arises, additional turbulence is generated due to the vibration of the surface, and the service life of the coatings is shortened. “Viscous” instability is apparently not so dangerous, because it appears in the form of static deformation of the coating and can be suppressed at a low viscosity by the interaction with the boundary layer.<sup>18</sup>

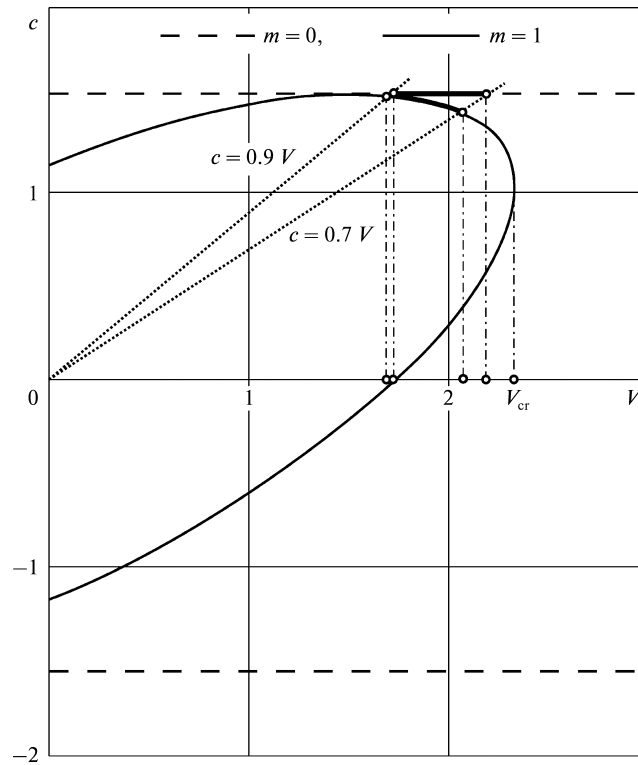


Fig. 13.

The second and third conditions, taken together, give the range of flow velocities in which the effective action of the coating is possible:

$$0.7V \leq c(k = 2.09, V) \leq 0.9V \tag{12.2}$$

In the case when  $m \neq 0$ , i.e., a dependence of  $c$  on  $V$ , this condition represents the inequalities for determining the range of the flow velocities  $V$ .

The fourth condition specifies the upper bound of the range of possible values of  $m$ , at which the coating is stable in the range of the velocities  $V$  obtained.

Condition (12.1) gives the range of coating thicknesses for assigned properties of the material.

We note two differences from the existing criteria.<sup>15</sup> First, due to the dependence of  $c$  on  $V$ , the solution of inequalities (12.2) for  $m \neq 0$  gives a range of velocities that includes smaller absolute values and is shorter than for  $m=0$ . In fact, a graphical solution of the dispersion equation containing  $c(V)$  and inequalities (12.2) in the example of  $\nu=0.5$  and  $m=0, 1$  is shown in Fig. 13, from which the preceding statement follows. Second, in the case in which the fluid (and, therefore, its density) is known (for example, when the motion of water is considered), along with the existing criteria,<sup>15</sup> there is an additional restriction, which is imposed on the minimal density of the coating that ensures stability. For example, solving inequality (12.2) for  $\nu=0.5$  (Fig. 13), we find:  $V=1.709 \dots 2.198$  when  $m=0$  and  $V=1.702 \dots 2.065$  when  $m=1$ . According to Fig. 5, we find for  $m=1$  that the coating is stable when  $V \leq 1.793$ , i.e., only the narrow velocity range  $1.702 \leq V \leq 1.793$  remains for stable operation. To ensure stability over the entire range, it is necessary that  $m \leq 0.5$ , i.e., in the case of water with  $\rho_f=1000 \text{ kg/m}^3$ , we obtain  $\rho \geq 2000 \text{ kg/m}^3$ . Furthermore, the choice of Young's modulus determines the dimensional velocity  $a_2$ , and it determines the range of dimensional flow velocities and coating thicknesses.

We present the results of selecting the properties of the coatings for  $\nu=0.475$  in dimensional form that were obtained with various values of the velocity  $a_2$  for flow in water. As was done previously,<sup>15</sup> to select the coating thickness, we use the relation (Ref. 26, Chapter 21, Section 1)

$$u_\tau = 0.172u \text{Re}_x^{-1/10}, \quad \text{Re}_x = \frac{Vx}{\nu_f} = \frac{V'a_2x}{\nu_f}$$

where  $V$  and  $V'$  are the dimensional and dimensionless velocities. We take the viscosity of water  $\nu_f=10^{-6} \text{ m}^2/\text{s}$  and the characteristic dimension  $x=1 \text{ m}$ . The results are shown in Fig. 14 in the form of regions on the  $V, \text{ m/s} - H, \text{ m}$  plane which satisfy criteria (12.1) and (12.2) for various values of the velocity of the transverse wave  $a_2, \nu=0.475$  and  $m=0, 1$ . As we can see, in all cases taking into account the dependence of the phase velocity on  $V$  results in a decrease in the operating range velocity, while the thickness range varies only slightly. From the stability condition we find approximately  $m \leq 0.5$ . We choose the smallest possible density of the material,  $\rho=2000 \text{ kg/m}^3$ . We take the working range of velocities from 17 to 20 m/s, and then it is necessary that  $a_2=10 \text{ m/s}$ . From the equality

$$a_2 = \sqrt{\frac{\mu}{\rho}} = \sqrt{\frac{E}{2(1+\nu)\rho}}$$

it follows that  $E=0.59 \text{ MPa}$ .

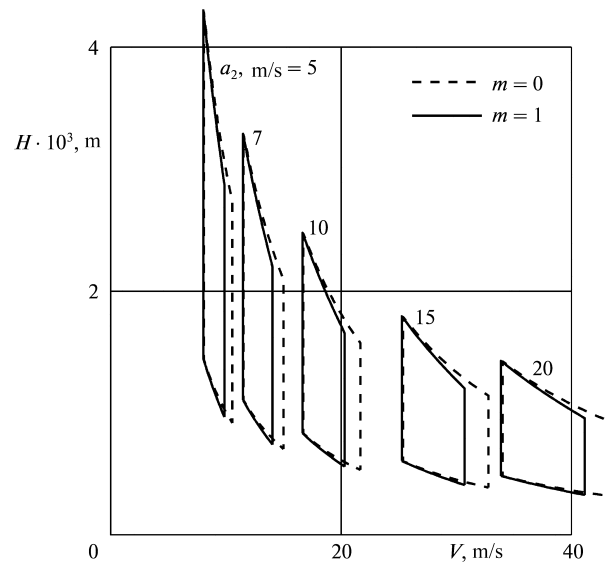


Fig. 14.

Thus, for the range of velocities of water from 17 to 20 m/s, the optimal coating is a layer of material having a thickness from 1 to 1.7 mm with

$$E = 0.59 \text{ MPa}, \quad \nu = 0.475, \quad \rho = 2000 \text{ kg/m}^3$$

### 13. Conclusion

It has been proved that a viscoelastic coating located under a moving fluid can lose stability when the velocity of the fluid  $V$  is sufficiently large. At the velocity  $V = V_0$ , which corresponds to elimination of the upstream travelling wave and its conversion into a downstream travelling wave, instability appears only when the coating has viscous properties. When the velocity  $V = V_{cr} > V_0$  is achieved, merging of the phase velocities of the two downstream travelling waves and the appearance of a stronger instability, which does not vanish in the purely elastic case, occur. While “elastic” instability of the coating is undesirable, since it can result in the additional generation of turbulence and destruction of the coating, “viscous” instability requires additional study. In the case of a small viscosity, this instability can be suppressed by the interaction with the boundary layer; otherwise, its appearance can also be tolerable, if the amplitude of the established bulging of the coating is small and does not exceed the thickness of the laminar sublayer, i.e., the coating remains hydraulically smooth.

It was shown that resonance wavelengths equal to 3–5 thicknesses of the coating, at which the interface performs strictly vertical vibrations, are scarcely influenced by the fluid. Evaluation of the influence of a moving fluid on the effectiveness of compliant coatings that are used to eliminate turbulent friction showed that the operating range velocity becomes smaller and an additional restriction on the density of the coating material for its operation in the stability region appears.

### Acknowledgements

I wish to thank V. M. Kulik and A. V. Boiko for discussing the results obtained.

This research was supported by the Russian Foundation for Basic Research (14-01-00052) and a grant from the President of the Russian Federation (MD-4544-2015.1).

### References

- Kramer MO. Boundary layer stabilization by distributed damping. *J Am Soc Naval Engineers* 1960;**73**(1):25–34.
- Carpenter PW, Garrad AD. The hydrodynamic stability of flows over Kramer-type compliant surfaces. Part 1. Tollmien–Schlichting instabilities. *J Fluid Mech* 1985;**155**:465–510.
- Carpenter PW, Garrad AD. The hydrodynamic stability of flows over Kramer-type compliant surfaces. Part 2. Flow-induced surface instabilities. *J Fluid Mech* 1986;**170**:199–232.
- Yeo KS. The stability boundary-layer flow over single and multi-layer viscoelastic walls. *J Fluid Mech* 1988;**196**:359–408.
- Savenkov IV. The suppression of the growth of non-linear wave packets by the elasticity of the surface around which flow occurs. *Comp Math Math Phys* 1995;**35**(1):73–9.
- Lingwood RJ, Peake N. On the causal behaviour of flow over an elastic wall. *J Fluid Mech* 1999;**396**:319–44.
- Wiplier O, Ehrenstein U. On the absolute instability in a boundary-layer flow with compliant coatings. *Europ J Mech B Fluids* 2001;**20**(1):127–44.
- Miles J. Stability of inviscid shear flow over a flexible boundary. *J Fluid Mech* 2001;**434**:371–8.
- Boiko AV, Kulik VM. Stability of flat plate boundary layer over monolithic viscoelastic coatings. *Dokl Phys* 2012;**57**(7):285–7.
- Xu S, Rempfer D, Lumley J. Turbulence over a compliant surface: numerical simulation and analysis. *J Fluid Mech* 2003;**478**:11–34.
- Luo H, Bewley TR. Accurate simulation of near-wall turbulence over a compliant tensegrity fabric. *Proc SPIE* 2005;**5757**:184–97.
- Fukagata K, Kern S, Chatelain P, Koumoutsakos P, Kasagi N. Evolutionary optimization of an anisotropic compliant surface for turbulent friction drag reduction. *J Turbulence* 2008;**9**(35):1–17.
- Semenov N. On conditions of modeling and choice of viscoelastic coatings for drag reduction. In: Choi K-S, editor. *Recent Developments in Turbulence Management*. Dordrecht: Kluwer; 1991. p. 241–62.
- Choi KS, Yang S, Clayton BR, Glover EL, Atlar M, Semenov BN, Kulik VM. Turbulent drag reduction using compliant surfaces. *Proc Roy Soc London Ser A* 1997;**453**:2229–40.

15. Kulik VM, Lee I, Chun NN. Wave properties of coating for skin friction reduction. *Phys Fluids* 2008;**20**(7):075109.
16. Reutov VP, Rybushkina GV. Hydroelastic instability threshold in a turbulent boundary layer over a compliant coating. *Phys Fluids* 1998;**10**(2):417–25.
17. Reutov VP, Rybushkina GV. Selection of the divergence waves on a model viscoelastic coating under a potential flow. *Phys Fluids* 2008;**20**(9):092108.
18. Duncan JH, Waxman AM, Tulin MP. The dynamics of waves at the interface between a viscoelastic coating and a fluid flow. *J Fluid Mech* 1985;**158**:177–97.
19. Yeo KS, Khoo BC, Zhao HZ. The absolute instability of boundary-layer flow over viscoelastic walls. *Theor Comp Fluid Dyn* 1996;**8**:237–52.
20. Viktorov IA. *Acoustic Surface Waves in Solids*. Moscow: Nauka; 1981.
21. Ewing WM, Jardetzky WS, Press F. *Elastic Waves in Layered Media*. New York: McGraw-Hill; 1957.
22. Sedov LI. *A Course in Continuum Mechanics, Vol. 3–4*. Groningen: Wolters-Noordhoff; 1972.
23. Kochin NE, Kibel' IA, Roze NV. *Theoretical Hydromechanics*. New York: Interscience; 1964.
24. Kulik VM, Boiko AV, Seoudi B, Chun NN, Lee I. Measurement method of complex viscoelastic material properties. *Int J Solid Struct* 2010;**47**(3):374–82.
25. Semenov BN. On the interference form of action of a viscoelastic boundary on near-wall turbulence. In: *Influence of Polymer Additions and the Elasticity of a Surface on Near-Wall Turbulence*. Novosibirsk: Nauka; 1978. p. 57–74.
26. Schlichting H. *Boundary-Layer Theory*. New York: McGraw-Hill; 1968.

Translated by P.S.